 doi:10.20944/preprints202202.0249.v1

# Modulation in the gene expression profile of astrocytes and monocytes by HIV-1 nef variants

**Sushama Jadhav[1,2]Prajakta Makar[3], Vijay Nema[1]**

[1] Indian Council of Medical Research, National AIDS Research Institute, 73, G Block,MIDC, Bhosari, Post Box No. 1895, Pune- 411 026, Maharashtra, India.
[2] Symbiosis International University, Lavale, Mulshi, Maharashtra, Pune, India
[3] InstituteofBioinformatics and Biotechnology (IBB),S.Phule Pune University, Pune

[*] **Corresponding Author:**

Dr. Vijay Nema,
Scientist E,
ICMR-NARI,
73, G Block, MIDC, Bhosari, Pune-411 026, Maharashtra, India
Tel: + 91 (020) 27331200;
Fax: + 91 (020) 27121071;
E-mail: vnema@nariindia.org

Preprints (www.preprints.org) | NOT PEER-REVIEWED | Posted: 21 February 2022 doi:10.20944/preprints202202.0249.v1

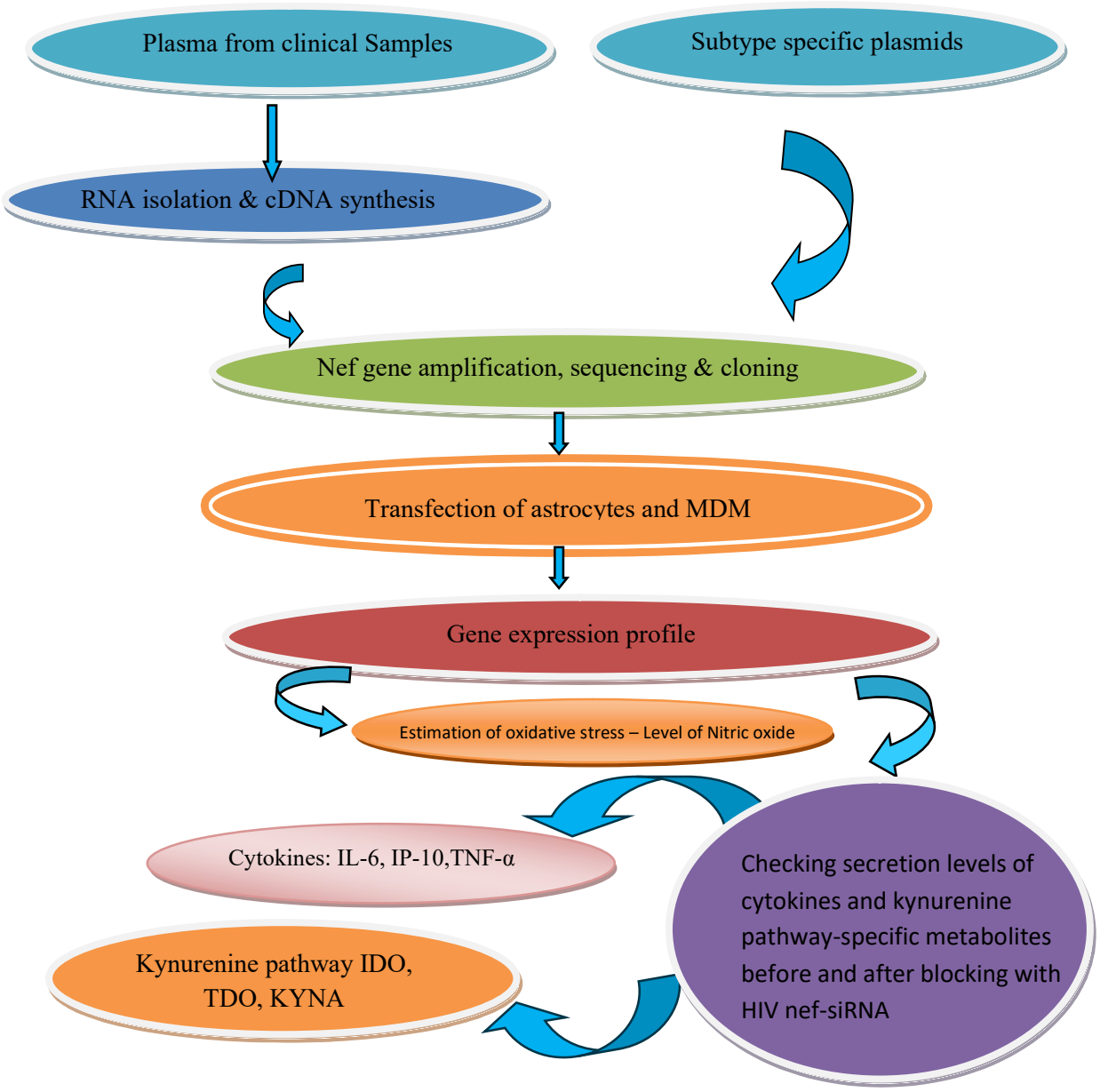


Figure 1: Schematic flow of experimental design

 doi:10.20944/preprints202202.0249.v1

**Abstract:**

HIV-1 Nef is a multifunctional protein with well-known lethal properties. HIV infects various cells from the brain compartment and expressed nef is responsible for developing neuropathogenic potential. HIV-infected glial cells express nefvirotoxinand stimulate the cascade of various pathways to activate uninfected cells to release neurotoxic elements damaging cells themselves. A lot of genetic variabilities of this protein have been reported from patients with HIV-associated neurocognitive disorders. To determine the neurotoxic potential of subtype-specific nef plasmids and nef plasmids of clinical samples with and without HAND were transfected in normal human astrocytes (NHA) and monocyte-derived macrophages (MDM) using nef-pCMV-HA plasmid constructs. Supernatants from subtype-specific Nef plasmids indicated the upregulation of proinflammatory cytokines. The induced expression might be due to the nef genetic variability or variations in the transfection efficiency and expression levels of nef.The mRNA expression of IL-6, IP-10, and TNF-α indicated upregulation of 5.0-fold in NHA and 3-fold in MDM with respect to empty vector control transfection. Further, the kynurenine metabolites were also assessed from culture supernatants of NHA and MDM indicating the upregulation of IDO and KYNU in NHA by 3.0-fold and 3.2-fold in MDM.The expression levels of nef and cytokines at the translational level were confirmed by western blotting and bio-plex Pro cytokine estimation assay respectively along with controls expressing green fluorescent protein (GFP).The oxidative stress was also found to be elevated as compared to control cells as determined by the estimation of nitric oxide from the culture supernatant to confirm the neurotoxic potential of HIV nef plasmids. The downregulation in the levels of cytokines, as well as kynurenine metabolites, was observed in culture supernatants after blocking the expression of nef using HIV nef siRNA. Phylogenetic analysis of Nef sequences indicated subtype C predominance except one sequence showing the partial sequence of HIV-1 subtype B sequence forming BC recombinant. The upregulation in the cytokine and pathway-specific metabolites might be linked with the neurotoxic potential of HIV-1 Nef leading to neuropathogenesis. In conclusion, the variation in the transfection efficiency, nef expression levels, and the genetic variability of Nef might be responsible for upregulating the expression levels of cytokines and kynurenine metabolites in astrocytes and MDM.

**Keywords:** HIV Nef, neurotoxicity, inflammatory cytokines, kynurenine metabolite

Preprints (www.preprints.org) | NOT PEER-REVIEWED | Posted: 21 February 2022 doi:10.20944/preprints202202.0249.v1

## 1. Introduction:

HIV-1 infection is reported to be a tremendous public health problem globally. There are approximately 1.7 million new infections and 680 thousand deaths due to AIDS-related illnesses by the end of the year 2020, while 37.7 million individuals are living with HIV infection [1]. Antiretroviral therapy (ART) is a standard therapy for HIV infection to help in the reduction of viral load and prolong life expectancy, and 27.5 million [26.5 – 27.7] infected individuals accessed ART in 2020 [1]. Although there is success on ART achieved so far for treating people with HIV infection, still there is a need for a safe, cost-efficient, easily accessible, and effective vaccine to attain a global control on the HIV pandemic [2]. Moreover, efficient deliverance of cART to the central nervous system is another hurdle. Due to such problems, enhanced viral load has been observed in the CNS developing HIV-associated neurocognitive disorders (HAND). Apart from this, one of the significant obstacles followed to date is the genetic variability of this virus which plays a central role in the progression of HIV infection towards neurological complications [3]. These complications were further identified under the umbrella of HIV-associated neurocognitive disorder. HIV-associated neurocognitive disorder (HAND) cases were found to be associated with recurrent neuroinflammation following neuronal damage and ultimately developing into HIV-associated dementia (HAD), which is a severe stage of the HAND [4,5]. Since 2005, the International HIV Dementia Scale (IHDS) [6] has been used widely as a screening tool to understand the prevalence of HAND. Another tool like Frascati criteria is used to standardize research criteria for HAND [7]. Though several publications have reported substantial progress due to ART, it still requires further improvement. Apart from this, neuronal cell death is frequently observed in the brains of HIV-1 positive individuals irrespective of ART regimen [8]. The direct effect of HIV-1 infection in the brain is due to the neurotoxicity of the virus [9] as well as due to virally encoded proteins like gp120 [10] transactivator of transcription (Tat) [11,12] and negative factor (Nef) [13,14].

Among various proteins, *Nef* is one of the most variable genes of HIV-1 [15] and remains an important factor for developing AIDS and ultimately progressing towards HAND. [16-18]. It translates into a 27 to 35 kDa protein expressed in the initial phase of viral replication, and it is expressed by latently infected cells and astrocytes [19]. Nef is highly neurotoxic, and Nef by itself is enough to yield oxidative stress, axon degeneration, and BBB damage [20]. Moreover, HIV Nef has numerous functions, including enhancement of viral infectivity and viral

 doi:10.20944/preprints202202.0249.v1

replication, [21] modulation of cell-surface receptors like down-regulation of CD4 receptor, [22] up-regulation of CD74, [23] down-regulation of HLA class I (HLA-I), [24] cellular signaling pathways affecting the intracellular organization [25]. These exchanges are linked with disease development and are associated with various motifs like N-Myristoylation, Proteolytic Cleavage region, Proline-rich motif, acidic region, dileucine, and FPD motif [26]. The mutations at functional regions of HIV-1 Nef protein could be associated with the disruption in the overall functioning of the protein and thus responsible for significant disease progression and pathogenesis in HIV-1 infected hosts [27]. Few of these functions are possible due to the nef protein's highly conserved amino acid motifs, while antigenic variability is still observed, which hinders developing an effective vaccine.

In addition to the viral and host genetic factors, certain factors are integral to the pathways modulating the disease condition drastically. Various metabolites of the kynurenine pathway, including kynurenine and quinolinic acid, are neurotoxic and elevated in HIV dementia patients. The viral proteins tat and nef induce such metabolites of the kynurenine pathway in macrophages which could be reversed after treatment with various anti-viral agents. Furthermore, neurotoxicity caused due to the metabolites of the kynurenine pathway had shown an association with HIV-associated neurocognitive disorder. It is obvious to link additional physiological activities like change in behavior, sleep, body temperature, and mood swings with this disorder [28]. The association of tryptophan metabolism with neurotoxicity is evidenced so far with the production of nicotinamide adenine dinucleotide and other neuroactive intermediates following the kynurenine pathway [29]. Most of the kynurenine pathway intermediate metabolites like kynurenine (KYN), kynurenic acid (KYNA), 3-hydroxykynurenine (3-HK), picolinic acid (PIC), and quinolinic acid (QUIN) are found to be induced in astrocytes, macrophages, and microglia due to cytokines triggered after their exposure to various HIV viral proteins.

Thus, the genetic diversity of HIV also plays an essential role in defining the subtype of the virus responsible for modulating various functions of various proteins at the translational level. The phylogenetic analysis determines the subtype identity to understand HIV transmission dynamics for effective HIV control [30]. Furthermore, HIV-1 genetic variability also influences diagnosis and measure of HIV viral load in-vivo. Hence, in-vitro studies on the transfection of subtype-specific HIV *nef* plasmids need to be explored.

Preprints (www.preprints.org) | NOT PEER-REVIEWED | Posted: 21 February 2022 doi:10.20944/preprints202202.0249.v1

In the present study, we have studied the inflammatory potential of HIV nef virotoxin by constructing the plasmids of the *nef* gene from clinical samples as well as the subtype-specific *nef* gene. The transfection of different concentration of nef and GFP control plasmid was done to determine the transfectionefficiency for performing transfection with nef plasmids of actual clinical samples. These plasmid constructs were transfected in the astrocytes and monocyte-derived macrophagesand studied the modulation in the secretion profile of proinflammatory cytokines and metabolites of the kynurenine pathway before and after blocking the expression of *Nef* with nef specific siRNA in *in-vitro* experiments.

The cytokine secretion profile was assessed using bio-plex Pro cytokine estimation assay after transfection of astrocytes and MDM with HIV Nef. At the same time, Real-time PCR was used to understand the intracellular expression profile of various genes at transcriptional levels. Additionally, the neurotoxicity was also estimated by measuring oxidative stress with the help of nitric oxide levels from the culture supernatants.

**2.0 Results**

**2.1 Amplification and molecular characterization of HIV nef gene**

The optimized PCR protocol resulted in amplification of the *nef* gene (620 bp) covering full-length nef gene containing restriction sites at both ends. All the ten selected clinical samples and subtype-specific plasmids and DNA from HIV-negative healthy control were amplified for the nef gene for construction of plasmid by cloning nef amplicon in pCMV-HA vector. The amplification of the nef gene is depicted in Figures 2 and3.

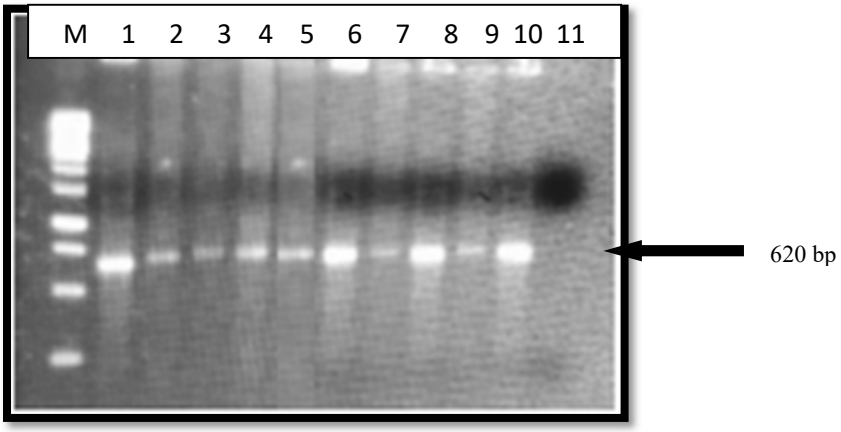


Figure 2: 1.2% Agarose gel electrophoresis of HIV-1 Nef gene amplified using PCR from 10 clinical samples and one normal healthy control DNA as a negative control (Lanes marked with M: 1 Kb DNA ladder, lanes marked with 1-10 are IHDS 1-10 Clinical samples, and lane marked with 11 is negative control)

Preprints (www.preprints.org) | NOT PEER-REVIEWED | Posted: 21 February 2022 doi:10.20944/preprints202202.0249.v1

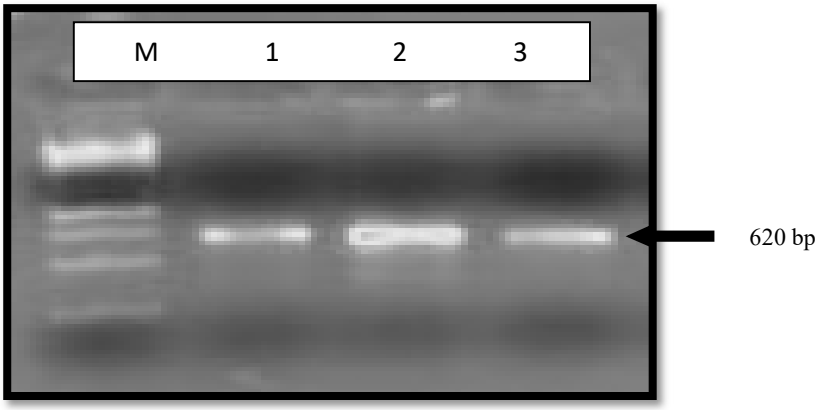


Figure 3: 1.2% Agarose gel electrophoresis of HIV-1 Nef gene amplifiedusing PCR from subtype specific Nef gene (M- 1 Kb DNA ladder, 1-pIndieC nef, 2- pNL4.3 nef, 3-pLconsnef)

We used the pCMV-HA vector and purified nef PCR products for the construction of the plasmids bycloning experiments. The cloning of the nef gene was confirmed by its amplification using a forward primer from the vector region and reverse primer of the nef gene. The full-length nef gene sequences were analyzed for the genetic variations and mutation patterns from the various functional motifs and presented in Table 3.

Table 3: Genetic variations and mutations in various functional motifs of study samples

| Patient Id | MGGKWS (1-6) | Arginine cluster (17,19,21,22) | Acidic cluster (62- 66) | PKC Binding region (76-85) | Basic residue for PAK Binding (105-106) | CD4 Downregulation (175-176) |
|---|---|---|---|---|---|---|
| IHDS-N1 | - | R21K | E66G | Y82F | - | D175E |
| IHDS-N2 | - | - | - | G84D | K105R | - |
| IHDS-N3 | - | - | - | - | - | - |
| IHDS-N4 | - | - | E66G | - | - | - |
| IHDS-N5 | - | - | E65 Deletion, E66D | Y82F | - | D175E |
| IHDS-N6 | - | R17K | E65G, E66D | - | K105R | D175E |
| IHDS-N7 | - | R22G | E66G | - | - | - |
| IHDS-N8 | - | - | E65G | G84S | - | D175E |
| IHDS-N9 | - | - | E65 Deletion | - | K105R | - |
| IHDS-N10 | - | R22Q | E65G | Y82F | - | D175E |

 doi:10.20944/preprints202202.0249.v1

The N-myristoylation motif (MGGKWSK), especially G2 of this motif, was an essential region for N-myristoylation and anchorage to the cell membrane conserved in both groups indicating the essentiality of docking of this amino acid portion to the cell membrane for viral entry. A cluster formed due to amino acid arginine at four locations, namely R17, R19, R21, R22, was found to be associated with membrane and responsible for downregulation of CD4. It was conserved at all the four places of the cluster in the dementia group except R21 is replaced by K21 in IHDS-N1, indicating either the nef mediated endocytosis or use of other receptors for viral entry as seen in an increased number of viral copies while in the non-dementia group the replacement of arginine at R17 by K17, R22 by G22 and R22 by Q22 in IHDS-N6, IHDS-N7 and IHDS-N10 respectively affecting the motif required for downregulation of CD4.

Apart from the arginine cluster, there are two more clusters namely phosphofurin acidic cluster sequences (PACS) like glutamate amino acid residue at position 62-65 and third motif VGFPV at amino acid position 66 – 70 were also responsible for nef induced vesicle secretion while there are certain amino acid residues like proline located at position 25, glycine-valine-glycine located at 29-31 and threonine at position 44 are responsible for regulating the secretion of vesicles responsible for blood-brain changes leading to neurotoxicity which are found to be conserved in both the study groups. This arginine cluster (R 17, 19, 21, 22) as well as another amino acid motif namely Q35, D36 is responsible for CD4 downregulation and both of these motifs are conserved in dementia and non-dementia group indicating its strong effect irrespective of disease status. Amino acid isoleucine is present at position 20 (Ile-20) in nef protein in 40% of the study samples and it was reported to be showing high viral copies in plasma which is in agreement with study samples except for two study samples. Three samples from each dementia as well as non-dementia group (IHDS-N1, IHDS-N3, IHDS-N4, IHDS-N7, IHDS-N8, and IHDS-N10 were showing methionine at position 20 which is reported to be a site for internal translation initiation and expression of non-myristoylated or truncated protein formation while two samples from each dementia as well as non-dementia group (IHDS-N2, IHDS-N5, IHDS-N6, IHDS-N9) were showing isoleucine at position 20 without affecting the full-length nef protein formation. This finding was free of related codons and there is no clinical association found with the polymorphisms observed in the functional regions.

Another reported specific proteolytic cleavage site at amino acid position 55 – 61 CAWLEAQ for viral protease within the virion is showing variability at position 59 by replacement of

 doi:10.20944/preprints202202.0249.v1

glutamate (E) by arginine (R) in IHDS-N1, IHDS-N2, IHDS-N4, IHDS-N6, IHDS-N7, IHDS-N7 and by polar uncharged glutamine in IHDS-N10 while keeping negatively charged glutamate (E59) conserved in IHDS-N3, IHDS-N5, IHDS-N9 and reported to be potential vaccine candidate. To be more precise, amino acids W57 and L58 are protease cleavage sites determining the molecular structure of nef and making partition into anchor and core domain. The amino acid tryptophan (W) at position 57 energizes the bendable PxxP motif found right from W57 till threonine (T) located at 81 forming the main proximity region with a groove of hydrophobic amino acids in the core domain. It is observed that both of these amino acids are preserved in all of our study samples. In the non-dementiagroup, there is the presence of Threonine (T) at position 72 in IHDS-N8 which is necessary for the SH3 binding area and some other molecules while it is replaced by arginine (R) in all remaining samples except IHDS-N4 which is showing lysine (K). T72 is also a destabilizing signature position however it is not showing association with the neurological condition for all study samples except IHDS-N8. Amino acid residues proline, valine, proline, arginine, lysine, aspartic acid phenylalanine, tryptophan, threonine at locations 73, 75, 76, 78, 83, 87, 91, 114, and 118 respectively are reported to be crucial for communication and play an important role in suppression of expression of CD4 molecule which is conserved in all study sequences, regardless of the neurocognitive status. Furthermore, well-preserved amino acids phenylalanine, proline, and aspartic acid at location 122–124 in consensus are mainly forming a loop and interacting with enzyme thereby influencing *nef*-mediated endocytosis and also suppressing the expression of CD4 and MHC1 molecules. This motif is conserved in all study sequences with and without dementia.

An endocytic ExxxLL signaling molecule containing two leucine (L) residues at locations 165 and 166 were very well-preserved in study sequences which are reported as vital for suppression of expression of CD4 molecule. Additional *nef* domain related with trafficking is negatively charged four glutamic acids (E) starting from amino acid position 62 which is conserved in most the samples except the presence of non-polar aliphatic amino acid residue glycine (G) in three samples from non-dementia group and absence of this amino acid in IHDS-N5 and IHDS-N9. At the end of proteolytic acidic cleavage region, at amino acid position 65, negatively charged glutamate (E) is conserved in IHDS-N1 to IHDS-N4, mutated in IHDS-N5, IHDS-N9 and replaced by glycine in IHDS-N6, IHDS-N8, and IHDS-N10 while at amino acid position 66, negatively charged glutamate (E) is conserved in IHDS-N2, IHDS-N3, IHDS-N8, IHDS-N9,

Preprints (www.preprints.org) | NOT PEER-REVIEWED | Posted: 21 February 2022 doi:10.20944/preprints202202.0249.v1

IHDS-N10 and replaced by non-polar aliphatic glycine (G) in IHDS-N1, IHDS-N4, IHDS-N7 and by negatively charged aspartate (D) in IHDS-N5, IHDS-N6. All these analyzed sequences were submitted to the GenBank database (Accession numbers: MT337374-MT337383)

The confirmed nef clones were also considered for the molecular characterization of sequences by analyzing sequences to understand the subtype by constructing a phylogenetic tree. The phylogenetic tree showed a formation of a single cluster of *nef* gene sequences reported from India along with study sequences indicating subtype C predominance except one Nef gene sequence showing the partial replacement of HIV-1 subtype B sequence forming BC recombinants (Figure 4).

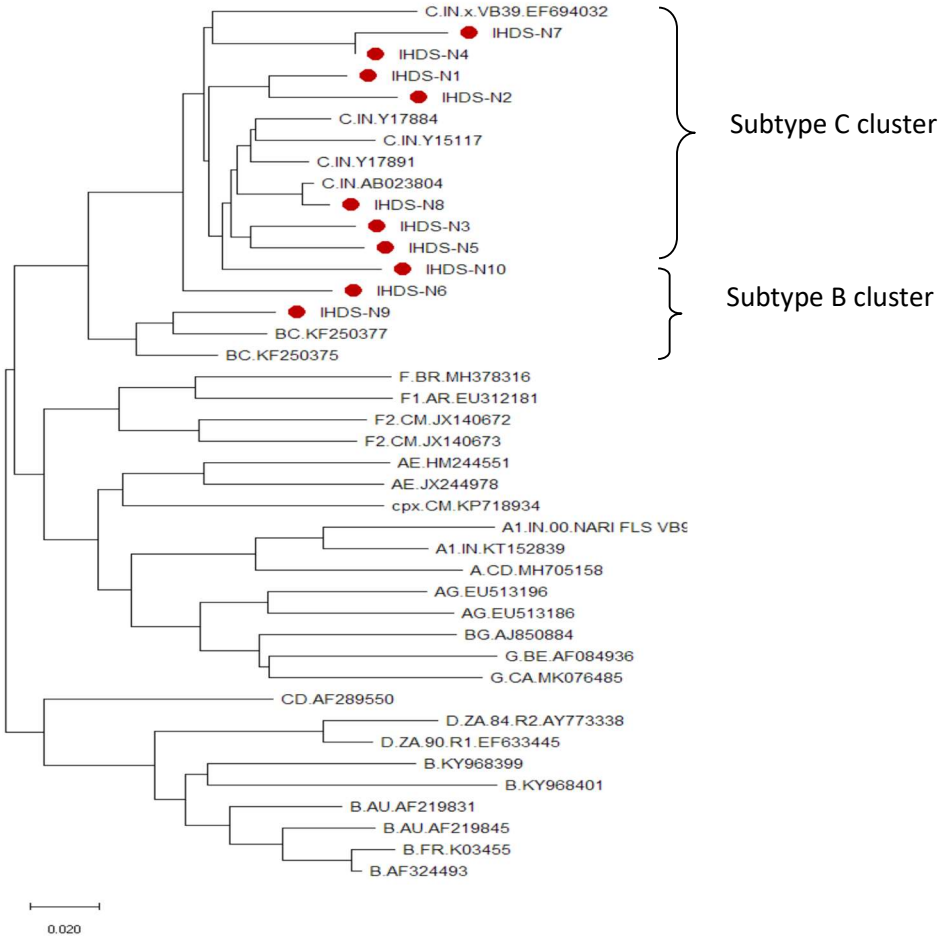


Figure 4: The phylogenetic tree of nef gene study sequences and other reported HIV-1 subtype-specific sequences and consensus sequences. The horizontal branch length represents the evolutionary distance, and the vertical distance represents relatedness. The study sequences are marked with a red do(), clustering with Indian HIV-1 Subtype C sequences.

Preprints (www.preprints.org) | NOT PEER-REVIEWED | Posted: 21 February 2022 doi:10.20944/preprints202202.0249.v1

### 2.2 Transfection of normal human astrocytes (NHA)

In vitro transient transfection of nef and GFP control plasmid confirmed the expression using various concentrations at the translational level. The data obtained from this experiment was helpful to finalize the concentration of plasmid to be used for subsequent transfection experiments. The western blot data was helpful for optimization of the concentration (A) and the protein levels from the cell lysates as well as supernatants has confirmed the transfection efficiency (B). The higher amount of nef protein observed in culture supernatant might be due to cell lysis and/or secretion of nef from transfected astrocytes.

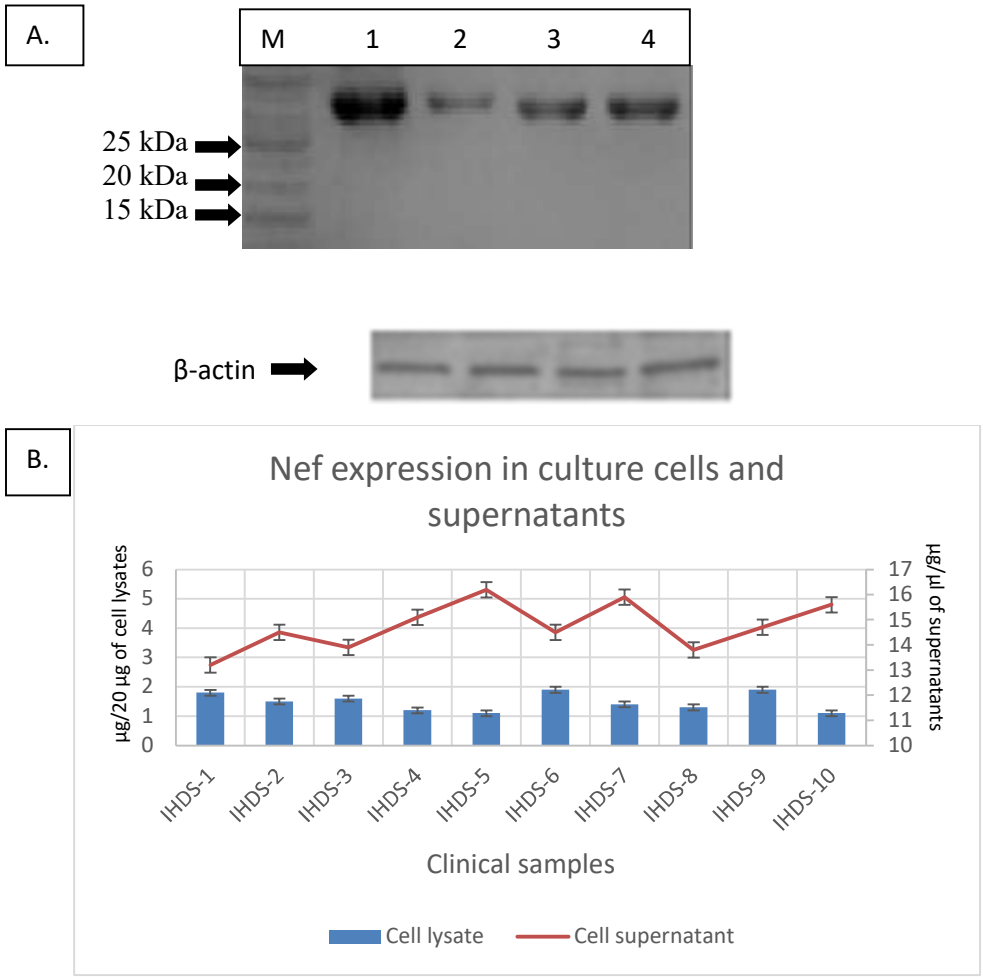


Figure No. 5 (A)Nefand GFP protein was expressed from astrocytes after transfection with different concentrations of nef and GFP control plasmids. First-line 'M' indicates the protein molecular weight marker, Line marked with 1 & 2 indicates expression of nef protein with 3 µg and 1 µg of plasmid transfected respectively. Line 3 & 4 indicate expression of GFP protein with 1 µg and 2 µg of control plasmid. Beta-actin was used as a loading control for cell lysates. (B)

Preprints (www.preprints.org) | NOT PEER-REVIEWED | Posted: 21 February 2022 doi:10.20944/preprints202202.0249.v1

Cells and supernatants were collected after transfection of astrocytes withall nef plasmids developed from clinical samples to determine the expression of nef.

**2.3Expression of inflammatory cytokines, and kynurenine metabolites in NHA and MDM**

The intracellularexpression levels of nef were determined by real-time PCR.To confirm the intracellular expression levels of nef, cytokines, and kynurenine metabolites, the RNA isolation was carried out from the culturedcells and supernatants before and after inhibition of the nef expression using nef siRNA in the transfection experiment. Real-time PCR estimated the kynurenine pathway-specific metabolites stimulated due to pro-inflammatory cytokines.

Initially, the cytokine expression levels of IL-6, IP-10, and TNF-α were determined before and after blocking the expression of nef using siRNA in astrocytes The mRNA levels of IL-6, IP-10, TNF-A after 6 hours of transfection in MDM were depicted in figure 6 A, Band in NHA were depicted in Figure 6 C, D estimated by real-time quantitative PCR (RT-qPCR) assay.

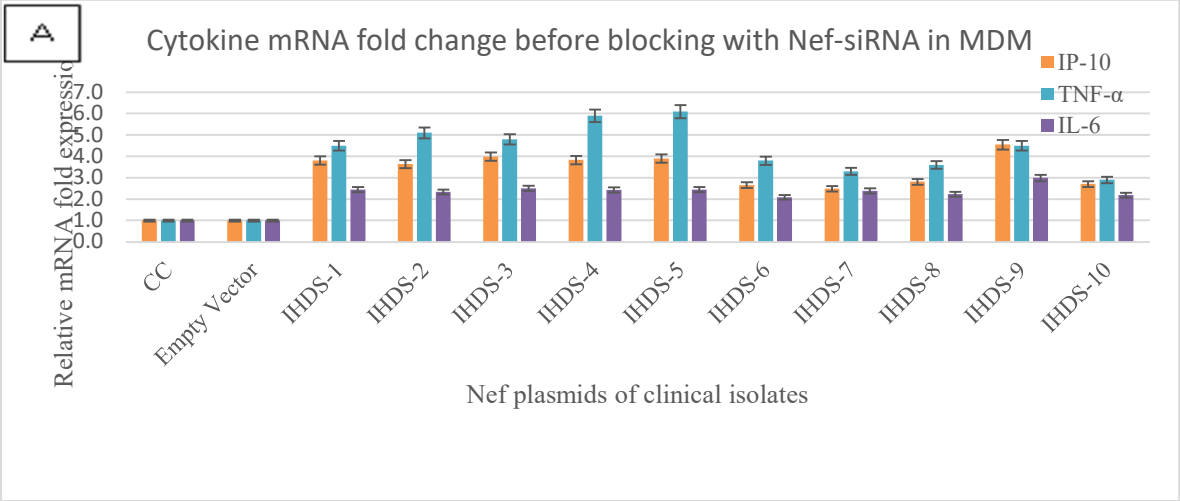


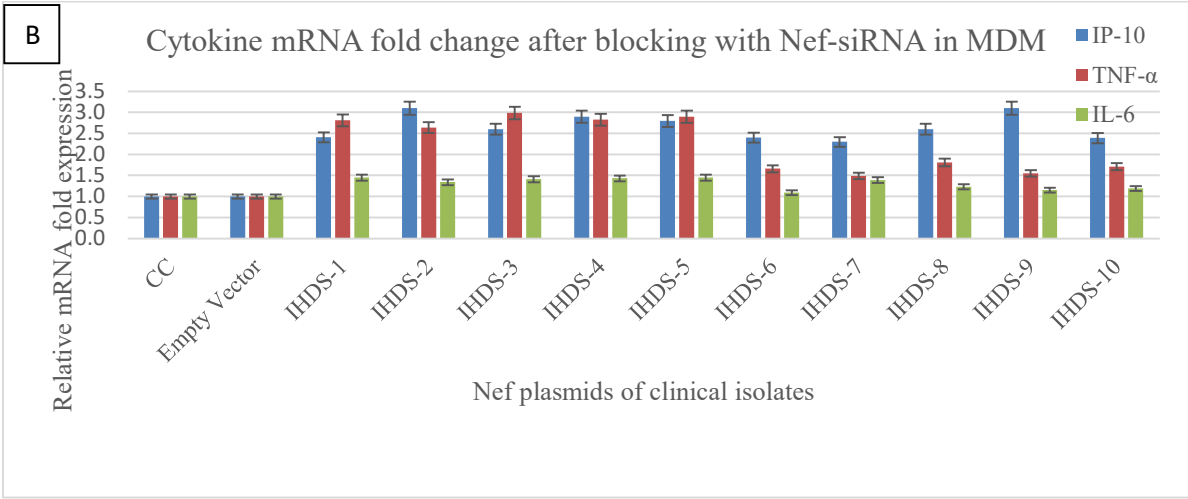

Preprints (www.preprints.org) | NOT PEER-REVIEWED | Posted: 21 February 2022 doi:10.20944/preprints202202.0249.v1

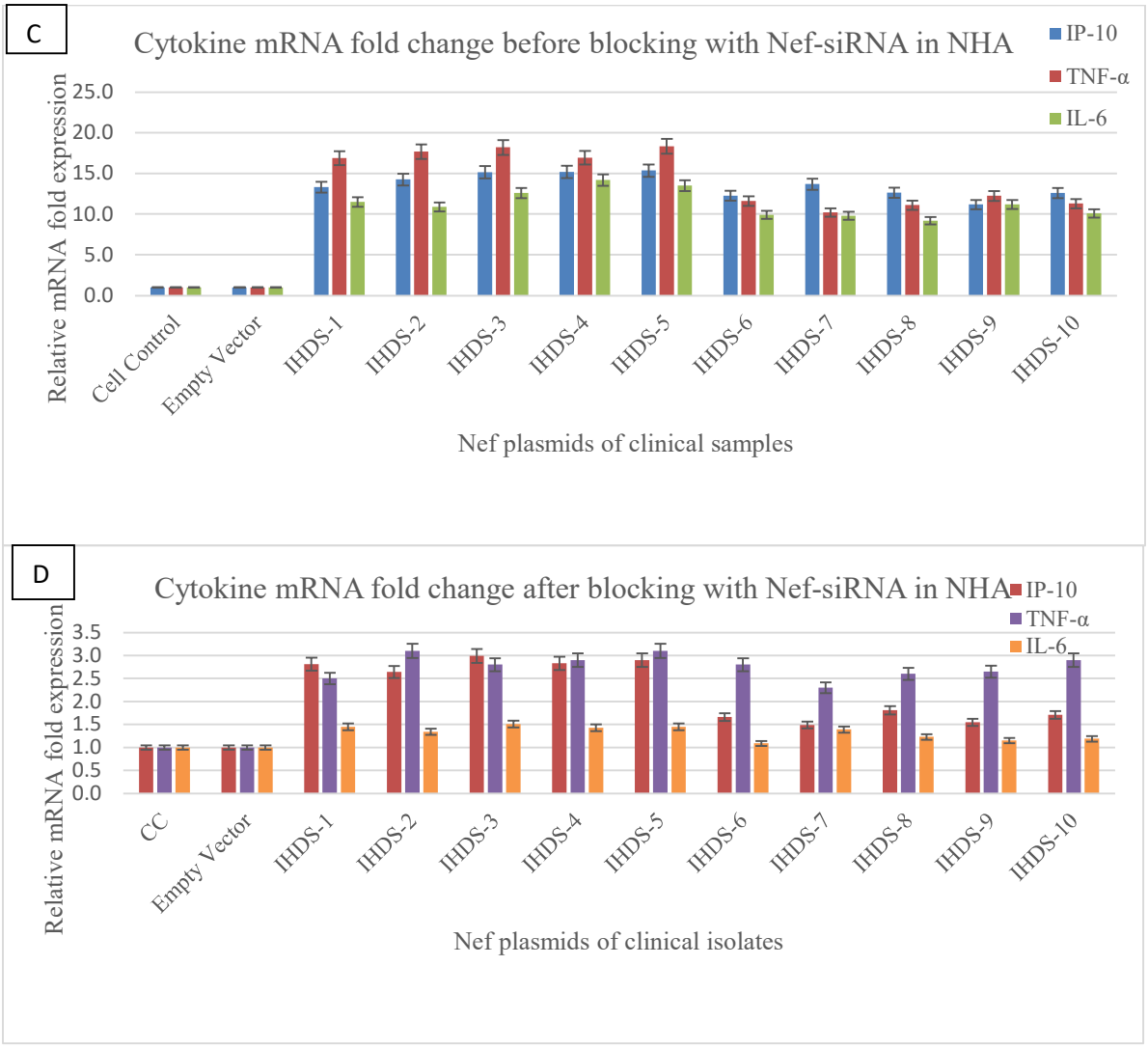


**Figure 6**: HIV-1 nef stimulates cytokine production in NHA and MDM. 2 x $10^5$ cells were seeded in a six-well plate and transfected with nef plasmid (constructed using clinical samples) using Lipofectamine 3000™. The cells were harvested after 6 hours, and RNA was isolated to determine cytokines mRNA expression at transcription level using real-time RT-PCR. The figures indicate relative fold change at mRNA expression level before and after blocking with Nef siRNA compared to empty vector-transfected control in NHA (A-B) and MDM (C, D), respectively.

The results indicated the comparison in the levels of pro-inflammatory cytokines at transcriptional level in the astrocytes and MDM after the transfection as well as after blocking the expression of nef with nef-specific siRNA. The study results displayed that in the nef plasmids of clinical samples, the expression level of the pro-inflammatory cytokines was reduced on an average by 5-fold in normal human astrocytes while 3-fold in monocyte-derived

Preprints (www.preprints.org) | NOT PEER-REVIEWED | Posted: 21 February 2022 doi:10.20944/preprints202202.0249.v1

macrophages. At the same time, the subtype-specific nef plasmids depicted the expression levels of cytokines around 5-fold, which was comparable with expression levels of astrocytes. The comparison was observed with a significant difference in cytokine expression levels in astrocytes and monocyte-derived macrophages. The determination of expression at transcriptional levels was carried out in duplicate and the mean values were considered for the analysis.

Additionally, the cytokine levels at the translational level were assessed by a Bio-Plex Pro assay using the culture supernatant from NHA before and after blocking with siRNA in duplicate and the results are depicted in figure 7 A & B. The cytokine levels from the supernatants of MDM were not assessed due to the unavailability of kit reagents of the Bio-Plex Pro assay.

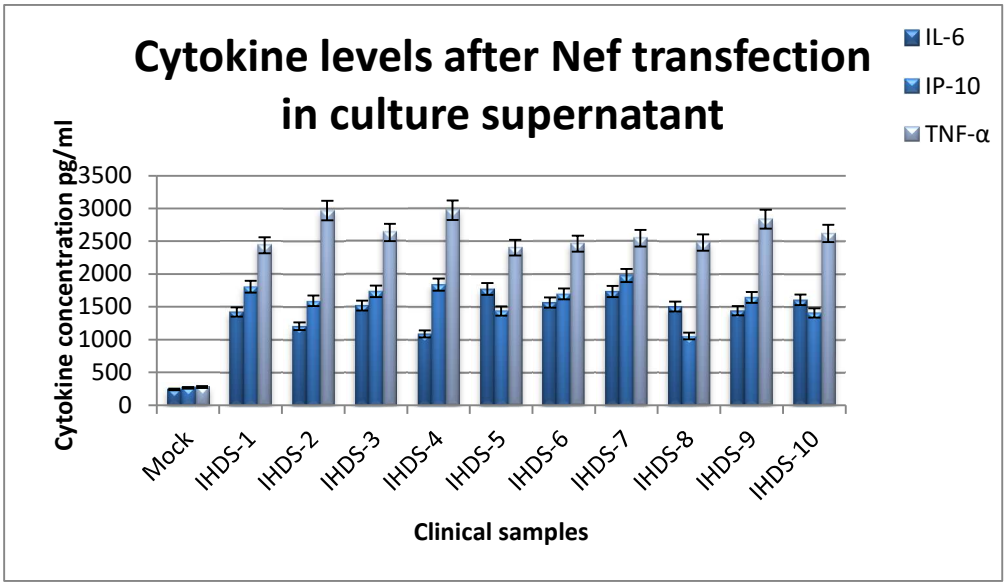


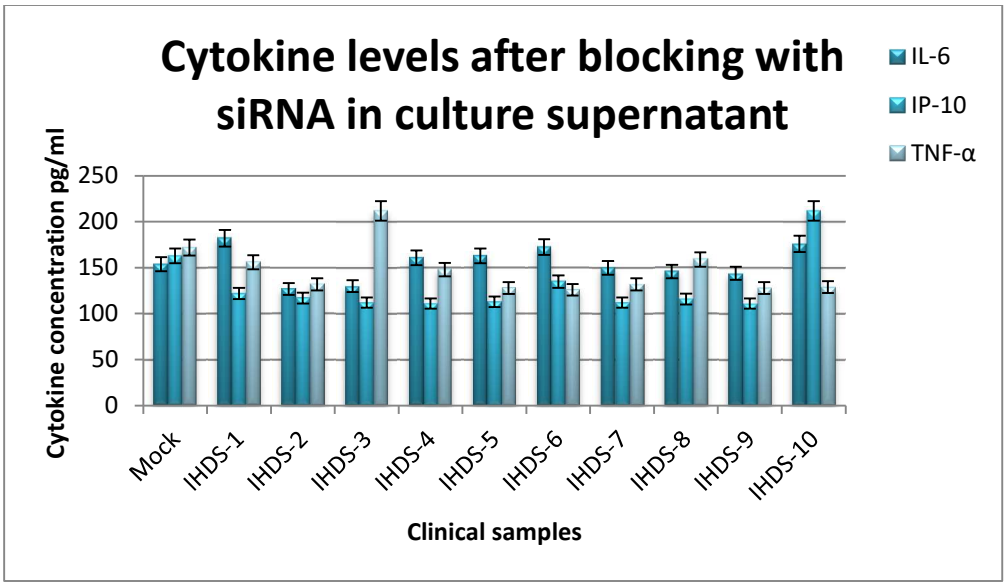

Preprints (www.preprints.org) | NOT PEER-REVIEWED | Posted: 21 February 2022 doi:10.20944/preprints202202.0249.v1

**Figure 7**: Cytokine levels estimated using Bio-Plex Pro assay (Biorad) 2 x $10^5$ cells were seeded in a six-well plate and transfected with nef plasmid (constructed using clinical samples) using Lipofectamine 3000™. The culture supernatants were used to determine cytokines levels at the translational level using the Bio-Plex Pro assay. Figure 7 (A & B) indicates concentration of cytokine levels before and after blocking with Nef siRNA along with NHA cell control (A & B). Additionally, we have determined the cytokine expression levels for the subtype-specific nef plasmids in normal human astrocytes. (Figure 8)

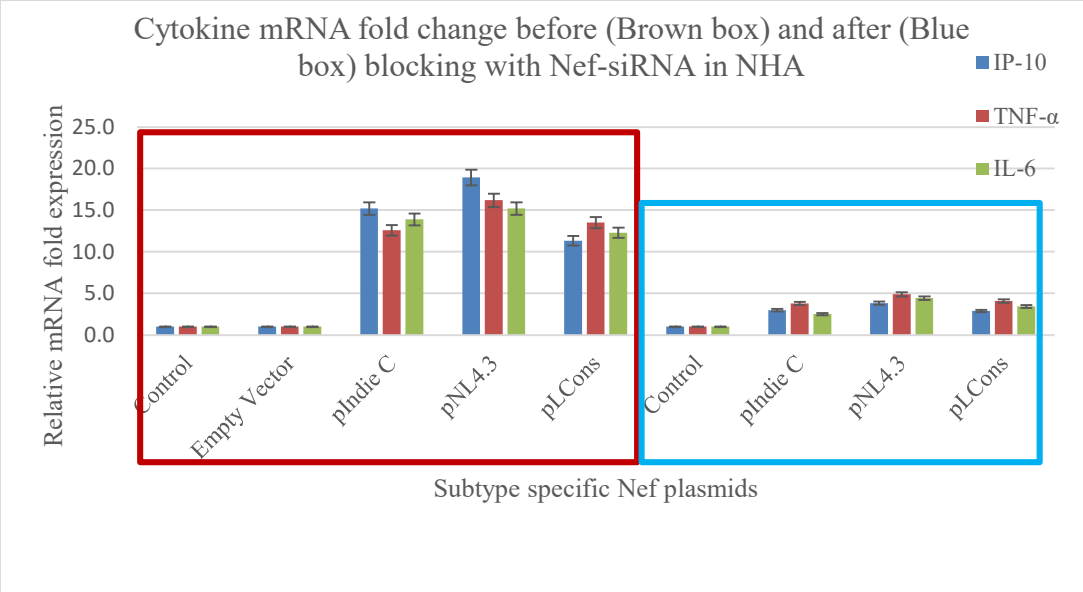


**Figure 8:**HIV-1 nef stimulates cytokine production in normal human astrocytes. 2 x $10^5$ cells were seeded in a six-well plate and transfected with nef plasmid (constructed using subtype-specific plasmids viz pIndieC for subtype C, pNL4.3 for subtype B, and consensus sequence of subtype C (pLconsnefSN) using Lipofectamine 3000™. The cells were harvested after 6 hours, and RNA was isolated to determine cytokines mRNA expression at transcription level using real-time RT-PCR. The figures indicate relative fold change at mRNA expression level concerning empty vector-transfected control in NHA.

To find out the impact of HIV nef transfection on kynurenine pathway-specific metabolites at transcriptional level, we have analyzed the expression of these genes. The kynurenine pathway-specific genes (IDO and KYNU) expression was relatively higher before blocking the expression of HIV nef clinical samples and subtype-specific plasmids. The relative fold change in mRNA expression levels was analyzed by real time PCR and depicted in Table 4 (A, B), respectively.

Preprints (www.preprints.org) | NOT PEER-REVIEWED | Posted: 21 February 2022 doi:10.20944/preprints202202.0249.v1

A.

| | Before blocking | | After blocking | |
|---|---|---|---|---|
| Gene symbol | IDO | KYNU | IDO | KYNU |
| IHDS-1 | 3.2 | 2.4 | 1.3 | 1.5 |
| IHDS-2 | 2.8 | 2.6 | 0.9 | 0.7 |
| IHDS-3 | 2.0 | 2.1 | 0.5 | 0.2 |
| IHDS-4 | 2.9 | 3.8 | 1.4 | 0.5 |
| IHDS-5 | 2.2 | 2.5 | 1.3 | 0.8 |
| IHDS-6 | 3.9 | 2.8 | 0.8 | 1.2 |
| IHDS-7 | 2.2 | 3.5 | 0.2 | 1.3 |
| IHDS-8 | 2.3 | 3.8 | 1.2 | 0.9 |
| IHDS-9 | 6.5 | 5.6 | 2.7 | 2.8 |
| IHDS-10 | 2.8 | 3.0 | 0.8 | 1.3 |

B.

| | Before blocking | | After blocking | |
|---|---|---|---|---|
| Gene symbol | IDO | KYNU | IDO | KYNU |
| pIndieC | 3.1 | 2.2 | 1.2 | 1.1 |
| pNL 4.3 | 4.5 | 5.1 | 1.7 | 1.8 |
| pLconsnefSN | 2.9 | 2.1 | 0.5 | 0.2 |

Table 4: Relative fold change in the mRNA expression levels of KP metabolites in normal human astrocytes before and after blocking with siRNA. (A) The normal human astrocyte cultures were transfected with medium alone (control) and Nef plasmids of clinical samples (~2µg/well) and (B) subtype-specific nef plasmids. The nef-specific siRNA (50 nM) was used to block before transfection, and culture supernatants were taken to estimate IDO and KYNU in two different experiments. Data shown are fold change (ratio) of mRNA expression (sample versus control). The average value was considered to depict results from two separate experiments.

**2.3 Effects of HIV nef plasmids on the production of nitrite in normal human astrocytes**

Normal human astrocytes were transfected with HIV nef plasmids (~1 µg/well), and culture supernatants were subjected to nitrite quantification in duplicate. The data are expressed as mean ± SEM from duplicate assays. One well from a six-well plate of cells was incubated without nef plasmid,which was considered control. ($P<0.03$)**Figure No. 9**

Preprints (www.preprints.org) | NOT PEER-REVIEWED | Posted: 21 February 2022 doi:10.20944/preprints202202.0249.v1

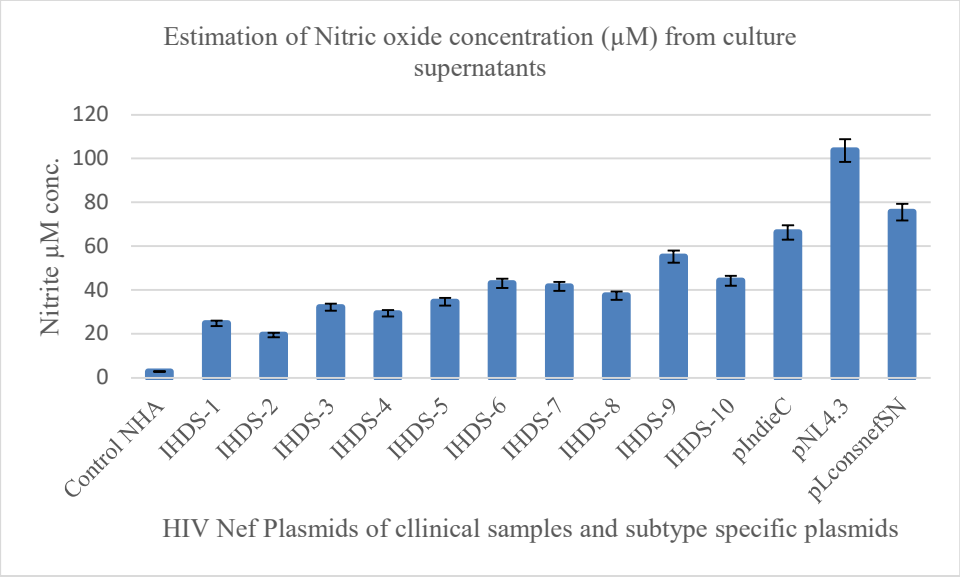


## 3.0 Discussion

As per the global scenario, most subtypes categorized under group M like A, B, C, and D contribute approximately 75% of the HIV pandemic. Among all regulatory proteins, HIV Nefis reported being a multifunctional and neurotoxic protein directly [31]. Additionally, nef protein is a critical factor for the development, progression of neuropathogenesis and is highly variable from various isolates of HIV. In the present study, astrocytes expressed nef demonstrating high cytokine expression levels that were mainly dependent on diversity in the sequence of HIV nef protein. The observations from the present study showed that intracellular expression of HIV nef and its heterogeneity contributed to the upregulation of cytokines and kynurenine pathway metabolites. The function of genetic heterogeneity within the nef gene is an essential pathogenic determinant, and that has been demonstrated in our study by differential stimulation of proinflammatory gene expression (IL-6, IP-10, and TNF-α) by subtype-specific Nef proteins[32, 33]. Furthermore, researchers are focusing on the role of nef protein in HAND pathogenesis as the abundant expression is reported from astrocytes of the brain compartment and exosomes from the blood and brain compartment [34 - 36]. HIV nef is essential for maintaining a high viral load and the progression of the disease [37]. HIV-1 Nef is mainly expressed in astrocytes, macrophages, and microglia[38]. At the same time,HIV nef-mediated neurotoxicity and neuroinflammation have been reported responsible for upregulation of proinflammatory cytokines and chemokines while down-regulation of cell surface markers, stimulating cell signaling molecules, disturbance of BBB, and enlarged levels of oxidative stress [39 - 40].

 doi:10.20944/preprints202202.0249.v1

Earlier studies have documented the higher expression of pro-inflammatory cytokines in CSF linked with HIV-associated dementia [41]. Elevated expression of pro-inflammatory cytokines and chemokines were linked with activation of various mechanisms accountable for HIV-1 mediated neuroinflammation. Moreover, different up-regulating signaling pathways like kynurenine, tryptophan metabolism, PI3K-PKCf, and p38b and p38d MAPK were also stimulated by HIV-1 Nef responsible for differentially regulating the IL-6 and IL-8 expression levels [42]. Among various types of cells from the brain, like perivascular macrophages, astrocytes, and microglia, astrocytes are abundantly present in the brain compartment. Around 19% of the cell population gets infected with HIV [43]. At the same time, astrocytes are infected in in-vitro cell-based assay due to virally encoded plasmids or replication-competent virus; however, they are inhibited by various immunosuppressive factors, like IDO is a rate-limiting enzyme of tryptophan metabolism.

In the present study, we have exposed normal human astrocytes and monocyte-derived macrophages to subtype-specific nef plasmids and nef plasmids constructed considering nef gene from clinical samples. We have observed the induction in the expression profile at mRNA and protein level, demonstrating a direct association between HIV-1 Nef and increased pro-inflammatory cytokines. To clarify the mechanisms responsible for HIV-1 Nef-mediated pro-inflammatory cytokine stimulation, we have expressed HIV-1 Nef in primary normal human astrocytes (NHA) and monocyte-derived macrophages (MDM) with a plasmid encoding HIV-1 Nef. As per the results reported previously with the astrocytic cell line, similar findings were observed, significantly matching cytokine production at mRNA and protein levels. Further, we tried to block the expression of HIV nef using nef siRNA. We showed its impact on the gene expression profile of kynurenine pathway-specific metabolites in primary normal human astrocytes and monocytic-derived macrophages. The fold change reduction after blocking with siRNA is significant. Thus, our study results demonstrate the involvement of different transcription factors responsible for HIV-1 Nef-mediated cytokine production and the participation of IDO and KYNU metabolites of the kynurenine pathway. The contribution of these pathways illustrates the possible role of siRNAs targeted against viral proteins and signaling molecules. It is possible to explore this approach further to treat neuroinflammation and cognitive deficits apparent in HAND patients. The critical evaluation of the gene expression profile indicated the impact of genetic diversity of HIV nef more significantly in normal human

 doi:10.20944/preprints202202.0249.v1

astrocytes (NHA) than in monocyte-derived macrophages (MDM). The overall relative mRNA expression of proinflammatory cytokines from the dementia group (IHDS 1 -5) is higher than the non-dementia group (IHDS 6-10), indicating the role of genetic diversity in gene expression profile. At the same time the presence of conserved residues at position P73, R78, D87, T118 amino acids are essential for the downregulation of CD4 receptor while conserved FPD amino acids at 122-124 are exposed as a loop and interact with human thioesterase, influencing nef mediated endocytosis and downregulation of CD4 and MHC1(Sequence alignment not shown). The observations from the current study correlate with previously observed findings and could be explored further with the involvement of other motifs from different genes and subtypes of HIV to correlate their role in neurotoxicity following neuroinflammation.

**4.0 Conclusion:** The outcome of this study suggested that HIV-1 nef-induced pro-inflammatory cytokines (IL-6, IP-10, and TNF-α), variations in the transfection efficiency, and levels of nef expression are probably the major causes of neurotoxicity and neuroinflammation in the culture-based assay. Furthermore, up-regulated expression of the IDO and KYNA mediated inflammation, oxidative stress-related to kynurenine pathway metabolites were observed in nef transfected astrocytes and MDM. Moreover, the reduced levels of expression at transcriptional and translational levels were observed against infection in *the in-vitro* cell-based assay after blocking the expression of nef with the help of nef siRNA transfection. Altogether, these results explored the role of HIV nef mediated inflammation in astrocytes and macrophages might be due to genetic variability of the nef gene or variations in the transfection efficiency and expression levels of nef. Future studies in this field may give success not only to the additional perceptive in treating neurodegenerative diseases but also to design the new strategies for upcoming neurological complications.

**5.0 Material and Methods:**

**5.1 Demographic details and clinical information of the study samples**

Institutional ethics committee approval [IEA] was taken before starting the proposed study. The assigned ethical committee protocol number is NARI-EC/2015-12 Version 1.0, 25/04/2015. The samples were considered for laboratory experiments after delinking the patient identities. Demographic information included various parameters like age, gender, nationality,

Preprints (www.preprints.org) | NOT PEER-REVIEWED | Posted: 21 February 2022 doi:10.20944/preprints202202.0249.v1

symptomatic/asymptomatic status, and risk behavior for the mode of HIV transmission for all HIV-positive individuals.

At the same time, a battery of neurological parameters like memory recall, motor speed, psychomotor speed responsible for identifying neurocognitive status is documented along with the history of ATT (anti-tubercular treatment) and ART. The CD4 cell count estimation was done by FACS Caliber (Becton Dickinson, USA) and documented as cells/µl. The plasma samples were analyzed to determine HIV-1 viral RNA copies using the COBAS system (Roche Diagnostic Systems, USA) and recorded as copies/ml. (Table 1) The current study was carried out to amplify *the nef* gene of the viral isolates from plasma samples of five HIV positive individuals with an IHDS score < 9.5, indicating the dementia status of the individual and five HIV positive individuals with an IHDS score >9.5 as non-dementia status (International HIV dementia scale). Additionally, HIV subtype-specific plasmids like pIndieC for subtype C, pNL4.3 for subtype B, and HIV Nef consensus sequence of subtype C pLconsnefSN (The reagent was obtained through the NIH HIV Reagent Program, Division of AIDS, NIAID, NIH contributed by Dr. Ron Swanstrom). After cell-based assays, the Nef gene was considered to amplify and analyze mutation patterns from the HIV-1 nef gene to explore its association with gene expression in astrocytes and monocyte-derived macrophages.

**Table 1: Demographic and clinical information of the individuals from the current study**

| IHDS* ID | Age | Sex | Mode of transmission | IHDS* Score | CD4 count (Cells/µl) | Viral load (Copies/ml) | Clinical findings |
|---|---|---|---|---|---|---|---|
| IHDS-1 | 45 | M | Heterosexual | 6.5 | 81 | 683885 | Pulmonary TB, Herpes Zoster, Oral Candidiasis |
| IHDS-2 | 26 | F | Heterosexual | 7.0 | 36 | 325290 | Herpes Zoster |
| IHDS-3 | 34 | M | Heterosexual | 7.5 | 45 | 2290000 | Herpes Zoster |
| IHDS-4 | 40 | M | Heterosexual | 8.0 | 60 | 412000 | Pulmonary TB |
| IHDS-5 | 35 | M | Heterosexual | 7.5 | 72 | 378577 | Pulmonary TB, Herpes Zoster |
| IHDS-6 | 29 | M | Heterosexual | 11.0 | 198 | 90100 | None |
| IHDS-7 | 42 | M | Heterosexual | 11.5 | 192 | 29386 | None |
| IHDS-8 | 34 | M | Heterosexual | 11.0 | 147 | 57086 | Herpes Zoster |
| IHDS-9 | 30 | M | Heterosexual | 12.0 | 193 | 68900 | Herpes Zoster |
| IHDS-10 | 47 | M | Heterosexual | 12.0 | 188 | 74845 | None |

*IHDS: International HIV Dementia Scale

Preprints (www.preprints.org) | NOT PEER-REVIEWED | Posted: 21 February 2022 doi:10.20944/preprints202202.0249.v1

**5.2 RNA isolation, amplification, and sequencing:** The isolation of viral RNA was carried out from ten plasma samples using Viral RNA Mini Kit (Qiagen, Studio City, CA). Approximately 500 ng of RNA was used to synthesize cDNA using a commercially available kit (Applied Biosystems, Foster City, CA) followed by nested PCR using full-length *nef* gene-specific primers. At the same time, HIV subtype-specific plasmids like pIndieC for subtype C, pNL4.3 for subtype B, and consensus sequence of subtype C were constructed by amplifying *nef*. The optimization of PCR was carried out with the help of primers designed to incorporate cutting sites of restriction enzymes in the second round of PCR. The primers for amplification covering the entire *nef* (8797-9414, HXB2) are used with high fidelity enzyme (Perkin Elmer) and other necessary reagents. Briefly, for the first-round *nef*-5 outer sense (5'ATTAGAGTTAGGCAGGGATA3'), and *nef*-6 outer antisense (5'CTGGTCTAACCAGAGAGACCCAGTAC3'), and for the second-round *nef*-7 inner sense (5' AAGAATTCGGATGGGTGGCAAGTGGTCAA3' and *nef*-8 inner antisense (5' ATAAGAAGCGGCCGCAGCAGTCTTTGTA3') primers were used for all amplifications with *Eco RI* and *Not I* restriction sites in forward and reverse primers respectively. The thermal cycling conditions were: 95°C for 10 min, followed by 30 cycles at 95°C for 1 min, 55°C for 1 min, and 60°C for 1 min for both the rounds of PCR [44]. The full-size amplicon of the HIV-1 *nef* gene comprising approximately 620 base pairs was confirmed by agarose gel electrophoresis for ten clinical samples as well as for subtype-specific plasmids. Amplified PCR products were purified by a gel extraction kit (Qiagen Studio City, CA) and sequenced using a Genetic analyzer. Genetic variability was determined by analyzing the sequences using the SeqScape software (v 2.7) and MEGA X software. The genetic variation and mutation pattern observed in various motifs of nef gene from clinical samples was evaluated to understand the impact of the mutation pattern on gene expression profile. At the same time, we have carried out subtype analysis of clinical samples based on phylogenetic analysis compared to reference subtype sequences.

**5.3 Construction of plasmids**

The plasmids were constructed using amplified nef gene of ten selected clinical samples as well as subtype-specific nef gene and transformed into pCMV-HA vector. To construct these plasmids, amplified and purified nef gene PCR products from clinical samples as well as subtype-specific plasmids were digested with *EcoRI and Not I* enzyme and cloned into the

Preprints (www.preprints.org) | NOT PEER-REVIEWED | Posted: 21 February 2022 doi:10.20944/preprints202202.0249.v1

pCMV-HA expression vector using T4 DNA ligase enzyme followed by the transformation in the bacterial system to construct plasmids of each nef gene for further experiments. To confirm the HIV nef plasmid construct, a PCR was carried out using pCMV-HA forward primer and nef gene reverse primer.

**5.4 Cell culture and transient transfection experiment**

For the present study, primary cells like normal human astrocytes (NHA) and THP-1 cell lines were obtained from Lonza Inc and the Institutional cell line repository, respectively. Normal human astrocytes are grown in cell culture medium like complete astrocytes medium (Gibco) containing N2 supplement and 10% Fetal bovine serum was used for cell propagation at 37°C and 5% CO2. At the same time, THP-1 cells were grown in RPMI 1640 media (Gibco) supplemented with 10% Fetal bovine serum (Gibco BRL) and penicillin-streptomycin solution of antibiotics (Invitrogen Inc.) and at gentamicin sulfate (Hi media) 37°C and 5% $CO_2$ environment.

Transient transfection of primary normal human astrocytes at a density of 2 x $10^5$ cells/wellwas carried out using 3 µg and 1 µg of nef plasmid construct with expression vector or 1 µg and 2 µg of GFP control plasmid in 500 µl of serum free medium using previously published protocol following replacement of medium containing 10% FBS. The cultured cells were incubated in $CO_2$ incubator at 37$^o$C. The cells were harvested for analysis of nef and GFP expression to determine transfection efficiency. The cells were lysed in lysis buffer and around 20 µg of cell lysates was loaded on 10% SDS-PAGE gel for resolving protein bands at 100 volts for 2 hrs maintaining temperature of the running buffer. The proteins were transferred to PVDF membrane using Trans Blot SD transfer apparatus without exceeding voltage of 25 V. The western blot was carried out as per the protocol published by Bhattacharya et al., 1998 by means of anti-nef monoclonal antibody and anti-beta actin primary antibody followed by suitable secondary antibody using chemiluminescent detection (Chemidoc XRS, Bio-Rad).

Subsequent transfection and treatments were carried out in 6 well or 12 well plates. After two to three passages and observance of the normal healthy appearance of the cells, a PMA reagent was added to transform THP-1 monocytes into monocyte-derived macrophages. In around 3-5 days, the monocytes were observed as transformed into macrophages. The confirmed plasmids of pIndieC, pNL4.3, pLconsnefSN were used for the transfection experiment. Transfections were carried out using Lipofectamine 3000 as per the manufacturer's instructions (Invitrogen Inc.,

Preprints (www.preprints.org) | NOT PEER-REVIEWED | Posted: 21 February 2022 doi:10.20944/preprints202202.0249.v1

Carlsbad, CA). About 50 nM HIV nef specific siRNA (GTGCCTGGCTAGAAGCACA) in medium without serum was added 24 hrs before HIV-1 Nef transfection. After 12 hrs, transfection media was changed with a fresh medium containing 10% serum.

The cells were trypsinized using 0.25% trypsin (Gibco) and seeded further for transfection experiment. Briefly, 2 x $10^5$ cells per well in 6 well plate were transfected with 1 – 2 µg of plasmid using 3 µl Lipofectamine in 1 ml plain medium without serum. After 6 hrs, the transfection medium was replaced by a fresh medium containing 10% FBS. Cell culture supernatants were collected from each experimental well at the indicated time intervals, followed by spinning at 3000 rpm for 10 minutes at 4ºC to remove floating cells and stored for further experiments.

**5.5 Real-time RT-PCR and multiplex cytokine assay.**

Synthesized cDNA from RNA isolated from cultured cells was used for real-time reverse transcriptase-polymerase chain reactions (RT-PCR) using 7900HT (Applied Biosystems Inc.) to estimate the mRNA expression levels. The reaction conditions included reverse transcription at 50ºC for 2 min, denaturation at 95ºC for 10 min, followed by amplification for 40 cycles (95ºC for 15 sec, 60ºC for 1 min). The IL-6, IP-10, TNF-α, IDO, KMO, QUIN primers were used for quantitative estimation. GAPDH was used as a housekeeping gene to normalize the expression of all genes using the 2(-ΔΔCT) method. Primers were synthesized with IDT technology from a commercial manufacturer (Table 2) and optimized annealing temperatures accordingly. The stored culture supernatants were used to estimate the concentration of cytokine proteins using a Bio-plex Pro assay system (Bio-Rad, Hercules, CA) according to the manufacturer's instructions. The expression of proteins was quantified using Bio-plex manager software v 5.0 along with the 5PL standard curve.The culture supernatants were considered for estimation of cytokine expression profile before and after blocking the expression of HIV nef to evaluate the change in the expression level of cytokines. A Biorad Pro Assay kit namely Bio-Plex Pro™ Human cytokine Grp I Panel 17-Plex, (IL-1β, IL-2, IL-4, IL-5, IL-6, IL-7, IL-8, IL-10, IL-12(p70), IL-13, IL-17, G-CSF, GM-CSF, IFN-γ, MCP-1, MIP-1 β, TNF-α was used to examine the effect of HIV nef exposure on gene expression in NHA. Briefly, the four-fold standard dilution series and blank and study samples were added in duplicate as mentioned in the kit protocol.

Preprints (www.preprints.org) | NOT PEER-REVIEWED | Posted: 21 February 2022 doi:10.20944/preprints202202.0249.v1

**Table 2: List of primers for real-time PCR**

| Target gene | Primer | Primer sequence 5' – 3' |
|---|---|---|
| GAPDH | Sense | 5'-ACCACCATGGAGAAGGCTGG-3' |
| | Antisense | 5'-CTCAGTGTAGCCCAGGATGC-3' |
| IL-6 | Sense | 5'-ACCCCAGGCAGACTACTTCT-3' |
| | Antisense | 5'-CCCAGATTGGAAGCATCCGT-3' |
| TNF-α | Sense | 5'-AGGCAACTTGCTCTCTCTCA -3' |
| | Antisense | 5'-CGGATCATGCTTTTGGTGCT-3' |
| IP-10 | Sense | 5'-CCTTCCTGTATGTGTTTGGA-3' |
| | Antisense | 5'-CCTGCTTCAAATATTTCCCT-3' |
| iNOS | Sense | 5′ TCCAGAAGCAGAATGTGACC-3′ |
| | Antisense | 5′-GGACCAGCCAAATCCAGT-3′ |
| IDO | Sense | 5'-ACCACAAGTCACAGCGCC-3' |
| | Antisense | 5'-CCCAGCAGGACGTCAAAG-3' |
| KYNU | Sense | 5'-GACTATTCCACCTAAGAACGGAGA-3' |
| | Antisense | 5'-ACAGGAAGACACAAACTAAGGTCG-3' |
| β-actin | Sense | 5' CCGTGACATCAAGGAGAA 3' |
| | Antisense | 5' GAAGGATGGCTGGAAGAG 3' |

### 5.6 Estimation of nitric oxide as a marker of neurotoxicity

Usually, the oxidative stress is measured as the nitric oxide synthesized in the cell culture supernatants using the EZAssay Nitric Oxide Estimation kit (Hi-media). The culture supernatants were diluted as per the instructions given in the protocol. The Ehrlich reagent I and II were used to estimate the nitric oxide present in the culture supernatant after transfection of the HIV nef plasmids constructed from clinical samples and subtype-specific plasmids in normal human astrocytes (NHA). The NO concentration was measured at 580 and 630 nm using ELISA Reader to calculate the nitric oxide synthesized. The assay was performed in duplicate, and the mean of two assays was considered to plot a graph of estimated nitric oxide in micromolar (µM) concentration.

 doi:10.20944/preprints202202.0249.v1

**5.7 Statistical Analyses**

The mean values and standard errors were calculated using GraphPad Prism 8 (Graph pad San Diego, CA, USA) software available in the institute. KP metabolite quantitation and cytokine levels were expressed as mean + SEM and plotted as a histogram with the analysis of significance using the student's unpaired T-test. A p-value of ($p < 0.05$) was considered statistically significant.

**6.0 Limitations of the work:**The limitation of this studyis the small number of samples and needs to be exploredfurther with other pathway-specific metabolites leading to neurotoxicity.

**Acknowledgments:** This study was carried out based on the topic of Ph.D. by the first author working with the ICMR family and who is registered (PRN 12049001008) under Symbiosis International University, Lavale, Pune, Maharashtra, India. The author acknowledges the support provided by the directors of the institute and all those who directly or indirectly were part of this study.

**Conflict of interest:** The authors declare no conflict of interest.

**Author contributions:** VN,SJ contributed to the conception and design of the study. SJ & PM performed assays,gathered the lab results,and analyzed data. SJ wrote the manuscript, VN helped in the manuscript's critical revision, and all authors read and approved the final manuscript.

**Funding:** The study was carried out using institutional intramural funds

**Institutional Review Board Statement**Institutional ethical (IEA) and scientific advisory committee (SAC) approval of the institute was taken before starting this work.

**Conflicts of Interest:** The authors declare no conflict of interest.

**References**

1. UNAIDS: Global HIV & AIDS statistics—2020 fact sheet. Available at www.unaids.org/en/resources/fact-sheet, accessed November 9, 2021.
2. Ng'uni T, Chasara C and Ndhlovu ZM (2020) Major Scientific Hurdles in HIV Vaccine Development: Historical Perspective and Future Directions. Front. Immunol. 11:590780. doi: 10.3389/fimmu.2020.590780
3. Hong S, Banks WA. Role of the immune system in HIV-associated neuroinflammation and neurocognitive implications. Brain Behav. Immun. 2015 Mar;45:1-12. doi: 10.1016/j.bbi.2014.10.008. Epub 2014 Oct 22. PMID: 25449672; PMCID: PMC4342286.

4. Clifford DB, Ances BM. HIV-associated neurocognitive disorder. Lancet Infect Dis. 2013;13(11):976–86.
5. Ghafouri M, Amini S, Khalili K, Sawaya BE. HIV-1 associated dementia: symptoms and causes. Retrovirology 2006; 3:28.
6. Sacktor N, Wong M, Nakasujja N, et al. The International HIV Dementia Scale: a new rapid screening test for HIV Dementia. AIDS 2005;19
7. Antinori A, Arendt G, Becker J, et al. Updated research nosology for HIV-associated neurocognitive disorders. Neurology 2007; 69:1789–1799.
8. Gaskill PJ, Miller DR, Gamble-George J, Yano H, Khoshbouei H. HIV, Tat and dopamine transmission. Neurobiol Dis. 2017; 105:51–73.
9. Spudich S. HIV and neurocognitive dysfunction. Curr HIV/AIDS Rep. 2013; 10(3):235–43.
10. Silverstein PS, Shah A, Weemhoff J, Kumar S, Singh DP, Kumar A. HIV-1 gp120 and drugs of abuse: interactions in the central nervous system. Curr HIV Res. 2012;10(5):369–83.
11. Green MV, Thayer SA. NMDARs adapt to neurotoxic HIV protein Tat downstream of a GluN2A-ubiquitin ligase signaling pathway. J Neurosci.2016; 36(50):12640–9.
12. Bruce-Keller AJ, Chauhan A, Dimayuga FO, Gee J, Keller JN, Nath A. Synaptic transport of human immunodeficiency virus-tat protein causes neurotoxicity and gliosis in rat brain. J Neurosci. 2003; 23(23):8417–22.
13. Bergonzi V, Calistri A, Salata C, et al. Nef and cell signaling transduction: possible involvement in the pathogenesis of human immunodeficiency virus-associated dementia. J Neuro-Oncol. 2009; 15(3):238–48.
14. Liu X, Shah A, Gangwani MR, Silverstein PS, Fu M, Kumar A. HIV-1 Nef induces CCL5 production in astrocytes through p38-MAPK and PI3K/Akt pathway and utilizes NF-kB, CEBP, and AP-1 transcription factors. Sci Rep. 2014; 4:4450.
15. Jubier-Maurin V, Saragosti S, Perret JL, et al. Genetic characterization of the nef gene from human immunodeficiency virus type 1 group M strains to represent genetic subtypes A, B, C, E, F, G, and H. AIDS Res Hum Retroviruses 1999; 15(1):23–32. doi:10.1089/088922299311673

16. Deacon NJ, Tsykin A, Solomon A, et al.Genomic structure of an attenuated quasi-species of HIV-1 from a blood transfusion donor and recipients. Science 1995; 270(5238):988–991
17. Kirchhoff F, Greenough TC, Brettler DB, Sullivan JL, Desrosiers RC. Brief report: the absence of intact nef sequences in a long-term survivor with nonprogressive HIV-1 infection. N Engl J Med 1995; 332(4):228–232. doi:10.1056/NEJM199501263320405
18. Daniel MD, Kirchhoff F, Czajak SC, Sehgal PK, Desrosiers RC. Protective effects of a live attenuated SIV vaccine with a deletion in the nef gene. Science 1992; 258(5090):1938–1941
19. Brack-Werner R. Astrocytes: HIV cellular reservoirs and essential participants in neuropathogenesis. Aids. 1999;13(1):1–22. Epub 1999/04/20. pmid:10207540.
20. Acheampong EA, Parveen Z, Muthoga LW, Kalayeh M, Mukhtar M, Pomerantz RJ. Human Immunodeficiency virus types 1 Nef potently induces apoptosis in primary human brain microvascular endothelial cells via the activation of caspases. J Virol. 2005;79(7):4257–69. pmid:15767427.
21. Ross TM, Oran AE, Cullen BR Inhibition of HIV-1 progeny virion release by cell-surface CD4 is relieved by expressing the viral Nef protein. CurrBiol 1999; 9(12):613–621
22. Garcia JV, Miller AD Serine phosphorylation-independent downregulation of cell-surface CD4 by nef. Nature 1991; 350(6318): 508–511. doi:10.1038/350508a0
23. Schindler M, Wurfl S, Benaroch P, et al. Downmodulation of mature primary histocompatibility complex class II and up-regulation of invariant chain cell surface expression are well-conserved functions of human and simian immunodeficiency virus nef alleles. J Virol 2003; 77(19):10548–10556.
24. Wang Yufei, Development of a human leukocyte antigen-based HIV vaccine, F1000 Research 874, Vol.7, doi.10.12688/f1000research.13759.1
25. Schwartz O, Marechal V, Le Gall S, Lemonnier F, Heard JM Endocytosis of primary histocompatibility complex class I molecules is induced by the HIV-1 Nef protein. Nat Med 1996; 2(3):338–342.
26. Stéphane Basmaciogullari and MassimoPizzato. The activity of Nef on HIV-1 infectivity, Frontiers in Microbiology, 20 May 2014 | https://doi.org/10.3389/fmicb.2014.00232
27. Meribe, SC, Hasan, Z., Mahiti, M. et al. Arch Virol 2015; 160: 2033. https://doi.org/10.1007/s00705-015-2480-5.

28. Munn, D.H. et al. 1998. Prevention of allogeneic fetal rejection by tryptophan catabolism. Science. 281:1191-93.
29. Moroni, F. 1999. Tryptophan metabolism and brain function: focus on kynurenine and other indole metabolites. Eur. J. Pharmacol. 375:87-100.
30. Castro-Nallar E, Perez-Losada M, Burton GF, Crandall KA. The evolution of HIV: Inferences using phylogenetics. Mol Phylogenet Evol 2012; 62:777–792.
31. Kumar M, Jain SK, Pasha ST, Chattopadhya D, Lal S, Rai A. Genomic diversity in the regulatory nef gene sequences in Indian isolates of HIV type 1: the emergence of a distinct subclade and predicted implications. AIDS Res Hum Retroviruses 2006; 22:1206–1219.
32. Trillo-Pazos et al., 2000
33. 40. Carlson JM, Brumme CJ, Martin E, Listgarten J, Brockman MA, Le AQ, et al. Correlates of protective cellular immunity revealed by analysis of population-level immune escape pathways in HIV-1. J Virol. 2012; 86(24):13202–16. https://doi.org/10.1128/JVI.01998-12 PMID: 23055555.
34. 41. Kinloch NN, Lee GQ, Carlson JM, Jin SW, Brumme CJ, Byakwaga H, et al. Genotypic and Mechanistic Characterization of Subtype-Specific HIV Adaptation to Host Cellular Immunity. J Virol. 2019; 93(1).
35. Saribas, A., Coric, Pascale and Bouaziz, Serge and Safak, Mahmut (2018), Expression of novel proteins by polyomaviruses and recent advances in the structural and functional features of agnoprotein of JC virus, BK virus, and simian virus 40, vol. 234, Journal of Cellular Physiology, doi 10.1002/JCP.27715
36. Reynolds J. L., Mahato R. I. (2017). Nanomedicines for the treatment of CNS diseases. *J. Neuroimmune Pharmacol.* 12 1–5. 10.1007/s11481-017-9725-x
37. Khan M. B., Lang M. J., Huang M. B., Raymond A., Bond V. C., Shiramizu B., et al. (2016). Nef exosomes isolated from the plasma of individuals with HIV-associated dementia (HAD) can induce Abeta(1-42) secretion in SH-SY5Y neural cells. *J. Neurovirol.* 22 179–190. 10.1007/s13365-015-0383-6
38. Kestler, H. W., 3rd et al. Importance of the nef gene for maintenance of high virus loads and development of AIDS. Cell 65, 651–662 (1991).
39. Gray LR, Turville SG, Hitchen TL, Cheng WJ, Ellett AM, Salimi H et al. HIV-1 entry and transinfection of astrocytes involves CD81 vesicles. PLoS One 2014; 9: e90620

40. Lehmann, M. H., Masanetz, S., Kramer, S. & Erfle, V. HIV-1 Nef upregulates CCL2/MCP-1 expression in astrocytes in a myristoylation calmodulin-dependent manner. J Cell Sci 119, 4520–4530 (2006).
41. Marantz, S. & Lehmann, M. H. HIV-1 Nef increases astrocytes sensitivity towards exogenous hydrogen peroxide. Virol J 8, 35 (2011).
42. Zheng, J. C. Et al. HIV-1 infected and immune-activated macrophages regulate astrocyte CXCL8 production through IL-1beta and TNF-alpha: involvement of mitogen-activated protein kinases and protein kinase R. J Neuroimmunol 200, 100–110 (2008).
43. Liu X, Kumar A. Differential signaling mechanism for HIV-1 Nef-mediated IL-6 and IL-8 in human astrocytes. Sci Rep. 2015 Jun 15;5:9867. doi: 10.1038/srep09867. PMID: 26075907; PMCID: PMC4467202.
44. Churchill MJ, Wesselingh SL, Cowley D, Pardo CA, McArthur JC, Brew BJ, et al. Extensive astrocyte infection is prominent in human immunodeficiency virus-associated dementia. Ann Neurol (2009) 66(2):253–8.10.1002/ana.21697.